European Journal of Pharmacology

Differential targeting of lysophosphatidic acid LPA1, LPA2, and LPA3 receptor signalling by tricyclic and tetracyclic antidepressants

--Manuscript Draft--

Manuscript Number:	EJP-65935
Article Type:	Research Paper
Section/Category:	Molecular and cellular pharmacology
Keywords:	antidepressants; human LPA receptors; receptor signalling; HEK293 cells
Corresponding Author:	Pierluigi Onali, M.D. ITALY
First Author:	Maria C. Olianas, PH.D.
Order of Authors:	Maria C. Olianas, PH.D.
	Simona Dedoni, Ph.D.
	Pierluigi Onali, M.D.
Abstract:	We previously reported that in different cell types antidepressant drugs activate lysophosphatidic acid (LPA) LPA1 receptor to induce proliferative and prosurvival responses. Here, we further characterize this unique action of antidepressants by examining their effects on two additional LPA receptor family members, LPA2 and LPA3. Human LPA1-3 receptors were stably expressed in HEK293 cells (HEK-LPA1, -LPA2 and –LPA3 cells) and their functional activity was determined by Western blot and immunofluorescence. LPA effectively stimulated the phosphorylation of extracellular signal-regulated protein kinases 1 and 2 (ERK1/2) in HEK-LPA1, -LPA2, and -LPA3 cells. The tricyclic antidepressants amitriptyline, clomipramine, imipramine and desipramine increased phospho-ERK1/2 levels in HEK-LPA1 and –LPA3 cells but were relatively poor agonists in LPA2-expressing cells. The tetracyclic antidepressants mianserin and mirtazapine were active at all three LPA receptors. When combined with LPA, both amitriptyline and mianserin potentiated Gi/o-mediated phosphorylation of ERK1/2 induced by LPA in HEK-LPA1, -LPA2 and -LPA3 cells, CHO-K1 fibroblasts and HT22 hippocampal neuroblasts. This potentiation was associated with enhanced phosphorylation of CREB and S6 ribosomal protein, two molecular targets of activated ERK1/2. The antidepressants also potentiated LPA-induced Gq/11-mediated phosphorylation of AMP-activated protein kinase in HEK-LPA1 and –LPA3 cells. Conversely, amitriptyline and mianserin were found to inhibit LPA-induced Rho activation in HEK-LPA1 and LPA2 cells. Moreover, mianserin failed to mimic LPA-induced reversal of astrocyte stellation, a response mediated by the G12/13-Rho pathway. These results indicate that tricyclic and tetracyclic antidepressants can act on LPA1, LPA2 and LPA3 receptor subtypes and exert differential effects on LPA signalling through these receptors.
Suggested Reviewers:	Jerold Chun Sanford Burnham Prebys Medical Discovery Institute jchun@sbpdiscovery.org Expert in LPA receptor pharmacology
	Gabor J Tigyi The University of Tennessee Health Science Center gtigyi@uthsc.edu Expert in LPA receptor pharmacology
	Mark Rasenick The University of Chicago College of Medicine raz@uic.edu Expert in antidepressant pharmacology

Editorial Office

European Journal of Pharmacology

Dear Editor,

attached please find the manuscript entitled: “Differential targeting of lysophosphatidic acid LPA_1, LPA_2, and LPA_3 receptor signalling by tricyclic and tetracyclic antidepressants” to be considered for publication in *European Journal of Pharmacology* as research paper.

Sincerely,

Pierluigi Onali, M.D.

Differential targeting of lysophosphatidic acid LPA_1, LPA_2, and LPA_3 receptor signalling by tricyclic and tetracyclic antidepressants.

Maria C. Olianas[1], Simona Dedoni, Pierluigi Onali[1]

Laboratory of Cellular and Molecular Pharmacology, Section of Neurosciences, Department of Biomedical Sciences, University of Cagliari, 09042 Monserrato (CA), Italy.

Corresponding author: Pierluigi Onali. e-mail: onali@unica.it

[1]Present address: ExplorePharma s.r.l., Edificio 5, Parco Scientifico e Tecnologico della Sardegna, Localita' Piscinamanna, 09010 Pula (CA), Italy.

Abstract

We previously reported that in different cell types antidepressant drugs activate lysophosphatidic acid (LPA) LPA_1 receptor to induce proliferative and prosurvival responses. Here, we further characterize this unique action of antidepressants by examining their effects on two additional LPA receptor family members, LPA_2 and LPA_3. Human LPA_{1-3} receptors were stably expressed in HEK293 cells (HEK-LPA_1, -LPA_2 and –LPA_3 cells) and their functional activity was determined by Western blot and immunofluorescence. LPA effectively stimulated the phosphorylation of extracellular signal-regulated protein kinases 1 and 2 (ERK1/2) in HEK-LPA_1, -LPA_2, and -LPA_3 cells. The tricyclic antidepressants amitriptyline, clomipramine, imipramine and desipramine increased phospho-ERK1/2 levels in HEK-LPA_1 and –LPA_3 cells but were relatively poor agonists in LPA_2-expressing cells. The tetracyclic antidepressants mianserin and mirtazapine were active at all three LPA receptors. When combined with LPA, both amitriptyline and mianserin potentiated $G_{i/o}$-mediated phosphorylation of ERK1/2 induced by LPA in HEK-LPA_1, -LPA_2 and -LPA_3 cells, CHO-K1 fibroblasts and HT22 hippocampal neuroblasts. This potentiation was associated with enhanced phosphorylation of CREB and S6 ribosomal protein, two molecular targets of activated ERK1/2. The antidepressants also potentiated LPA-induced $G_{q/11}$-mediated phosphorylation of AMP-activated protein kinase in HEK-LPA_1 and –LPA_3 cells. Conversely, amitriptyline and mianserin were found to inhibit LPA-induced Rho activation in HEK-LPA_1 and LPA_2 cells. Moreover, mianserin failed to mimic LPA-induced reversal of astrocyte stellation, a response mediated by the $G_{12/13}$-Rho pathway. These results indicate that tricyclic and tetracyclic antidepressants can act on LPA_1, LPA_2 and LPA_3 receptor subtypes and exert differential effects on LPA signalling through these receptors.

Keywords: antidepressants; human LPA receptors; receptor signalling; HEK293 cells.

1. Introduction

Lysophosphatidic acid (LPA) is a bioactive glycerophospholipid that acts through at least six distinct G protein-coupled receptors (GPCRs), termed $LPA_{1-6,}$ which are subdivided into the endothelial cell differentiation gene (EDG) family comprising LPA_{1-3}, and the P2Y purinergic receptor family including LPA_{4-6} (Tigyi, 2010; Yung et al., 2014; Kihara et al., 2014). Activation of LPA receptors regulates a wide spectrum of key intracellular signalling pathways, including mitogen-activated protein (MAP) kinase, phospholipase C, phosphatidylinositol-3 kinase / Akt, adenylyl cyclase and Rho pathways, by coupling to the heterotrimeric G proteins $G_{i/o}$, $G_{q/11}$, $G_{12/13}$, and G_s (Kihara et al., 2014; Stoddard and Chun, 2015). LPA and LPA receptors have been shown to control neurogenesis, development of vascular system, immunological responses and reproductive function (Yung et al., 2014, 2015). Moreover, LPA transmission is involved in diverse pathologic conditions, such as neuropsychiatric diseases, neuropathic pain, atherosclerosis, fibrosis and cancer (Schober and Siess, 2012; Yung et. al., 2015; Geraldo et al., 2021). However, relatively little is known on the effects of clinically used drugs on either central or peripheral LPA signalling.

We first reported that in CHO-K1 fibroblasts tricyclic and tetracyclic antidepressants activate endogenously expressed LPA_1 receptors to induce insulin-like growth factor-1 receptor transactivation, extracellular signal-regulated kinases 1 and 2 (ERK1/2) stimulation and mitogenesis (Olianas et al., 2015). We also showed that through the activation of LPA_1-coupled ERK1/2 signalling antidepressants protect glial cells from oxidative stress and hippocampal neurons from TNF-α-induced apoptotic cell death (Olianas et al., 2016, 2017, 2019). These studies demonstrated for the first time that the LPA_1 receptor could act as molecular target of different classes of antidepressants and suggested that this effect could contribute to the therapeutic actions of the drugs. The ability of antidepressants to activate LPA_1 was confirmed by independent investigations.

Thus, it was reported that in astroglial cells antidepressant-induced LPA_1 activation mediates the induction of glial cell line-derived neurotrophic factor (Kajitani et al., 2016). In rat brain capillaries the antidepressant amitriptyline and LPA have been found to reduce P-glycoprotein transport activity through LPA_1 and ERK1/2 (Banks et al., 2018). Recently, we reported that in human dermal and lung fibroblasts LPA_1 mediates profibrotic responses of antidepressants similar to those elicited by LPA, indicating that LPA_1 activation could also contribute to the adverse effects of the drugs (Olianas et al., 2020).

Although increasing information has accumulated concerning the antidepressant action on LPA_1 signalling, little is known about the effects of these drugs at the other members of the EDG family which share a high sequence homology to LPA_1. LPA_2 and LPA_3 display a more restricted tissue expression as compared to LPA_1 but are present in several human organs and have been shown to mediate crucial functions of LPA on cell survival, cell migration, and reproductive function (Kihara et al. 2014; Yung et al., 2014; Solis et al., 2021).

In the present study we investigated the actions of tricyclic and tetracyclic antidepressants on human LPA_1, LPA_2 and LPA_3 receptors stably expressed in human embryonic kidney cells (HEK)-293 and coupled to distinct signalling pathways.

2. Materials and Methods

2.1. Materials

Amitriptyline hydrochloride, clomipramine hydrochloride, imipramine hydrochloride, desipramine hydrochloride, mianserin hydrochloride, mirtazapine hydrochloride, nor-adrenaline hydrochloride (NA), 4',6-diamidino-2phenylindole dihydrochloride (DAPI), *Bordetella pertussis* toxin (PTX), and G 418 sulfate were obtained from Sigma Aldrich (St. Louis, MO, USA). 1-Oleoyl-lysophosphatidic acid (LPA) was purchased from Santa Cruz

Biotechnology (Dallas, TX, USA). Recombinant mouse basic fibroblast growth factor (FGF-2) was from ProSpec-Tany TechnoGene ltd (Ness Ziona, Israel). Ionomycin was from Calbiochem (La Jolla, CA, USA). The cyclic depsipeptide YM-254890 was kindly provided by Dr. Jun Takasaki, Yamanouchi Pharmaceutical Co. Ltd (Tsukuba, Ibaraki, Japan). The other reagents used were from Sigma-Aldrich.

2.2. Cell culture

Human embryonic kidney-293 (HEK-293) cells (Cell lines Service, Eppelheim, Germany) were grown in Dulbecco's modified Eagle's medium (DMEM)/Ham's F12 medium (1:1) supplemented with L-glutamine, 10 % foetal calf serum (FCS) and 0.5 % penicillin/streptomycin (P/S) (Sigma Aldrich) at 37 °C in a humidified atmosphere of 5 % CO_2 in air. HEK-293 cells overexpressing human LPA_1, (HEK-LPA_1), LPA_2 (HEK-LPA_2) and LPA_3 (HEK-LPA_3) receptors were generated by transfection with the respective human cDNAs cloned into pcDNA3.1 vector (UMR cDNA Resource Center, Rolla, MO, USA and cDNA Resource Center, Bloomsburg, PA, USA; www.cdna.org) using Lipofectamine 2000 as transfectant (Invitrogen/Life Technologies, Monza, Italy). Following transfection, stably transfected cell clones were selected by incubation for six-seven weeks with 1 mg/ml G 418 sulfate and subsequent screening for LPA-induced phospho-ERK1/2 stimulation. Positive clones were maintained in growth medium supplemented with 0.4 mg/ml G 418 sulfate.

HT22 hippocampal cells were generously provided by Dr. David Schubert (The Salk Institute, La Jolla, CA, USA). The cells were grown in DMEM medium supplemented with 10 % FCS and 0.5 % P/S at 37 °C in a humidified atmosphere with 5 % CO_2.

Chinese hamster ovary-K1 (CHO-K1) cells (American Type Culture Collection, Manassas, VA, USA) were grown in Ham's F12 medium containing 2 mM glutamine, sodium bicarbonate, 10 % FCS and 0.5 % P/S at 37 °C in a atmosphere with 5 % CO_2.

Frozen aliquots of astrocytes, prepared from cerebral cortex of newborn rats as previously described (Olianas et al., 2016) and stored in liquid nitrogen, were thawed and cultured in DMEM/Ham's F12 medium containing 10 % FCS and 0.5 % P/S at 37 °C in a atmosphere with 5 % CO_2.

2.3. Cell treatment

Unless otherwise specified, subconfluent cell cultures grown in six-well plates were serum-starved for either 16-24 h (HEK-293, CHO-K1 fibroblasts, and rat astrocytes) or 2 h (HT22 hippocampal cells). Thereafter, the medium was renewed, and the cells were incubated for 1 h before treatment with the test agents as indicated in the text.

2.4. Western blot analysis

Following exposure to the test agents, cells were washed in ice-cold phosphate buffered saline (PBS) (pH 7.4) and cell lysates were prepared by scraping the cells in ice-cold RIPA buffer containing PBS, 2 mM EDTA, 2 mM EGTA, 4 mM sodium pyrophosphate, 2 mM sodium orthovanadate, 10 mM sodium fluoride, 20 nM okadaic acid, 0.5 % phosphatase inhibitor cocktail 3, 1 % protease inhibitor cocktail (Sigma Aldrich), 1 mM phenylmethylsulphonyl fluoride (PMSF), 0.1 sodium dodecyl sulphate (SDS), 1 % Nonidet P-40 (pH 7.4) and 0.5 % sodium deoxycholate. Following sonication for 5 s at ice-bath temperature, protein concentration was determined by the Bio-Rad Protein assay kit (Bio-Rad Lab., Hercules, CA, USA). Aliquots of the cell lysates containing an equal amount of protein were subjected to SDS-polyacrylamide gel electrophoresis and then electrophoretically transferred to polyvinylidene difluoride membranes. Membranes were blocked with 5% non-fat dry milk (Santa Cruz Biotechnology), washed and incubated overnight at 4 °C with one of the following primary antibodies: rabbit polyclonal anti-phospho-ERK 1(Thr202/Tyr204) / ERK2 (Thr185/Tyr187) (cat. no. RA15002, Neuromics, Northfield, MN, USA) (1:10,000), rabbit polyclonal anti-ERK1/2 (cat. no. 9102, Cell

Signaling Technology, Beverly, MA, USA) (1:1000), rabbit monoclonal anti-phospho-AMP-activated protein kinase (AMPK) α subunit (Thr172) (cat. no. 2535, Cell Signaling Technology) (1:1000), rabbit polyclonal anti-AMPKα1/2 (sc-25792, Santa Cruz Biotechnology) 1:1000), rabbit polyclonal anti-Rho (cat no. 8789, Cell Signaling Technology) (1:667). Thereafter, the membranes were washed and incubated with horseradish peroxidase-conjugated goat anti-rabbit IgG (A 0545 Sigma Aldrich) (1: 15,000) for 1 h at room temperature. Immunoreactive bands were detected by using Clarity Western ECL substrate (Bio-Rad Lab.) and digital images were obtained by using either ECL Hyperfilm (Amersham) with Image Scanner III (GE Healthcare, Milan, Italy) or Luminescence Image analyzer LAS 4000 (FujiFilm, Tokyo, Japan). Band densities were determined by using the NIH ImageJ software (US National Institutes of Health, Bethesda, MD, USA). The density of the phosphorylated protein bands was normalized to the density of the corresponding total protein in the same sample, whereas active Rho was normalized to the density of total Rho determined in the same sample.

2.5. Immunofluorescence microscopy

Cells were plated and grown on glass coverslips precoated with 0.01% poly-L-lysine to 50-60 % confluency in 24-well plates. Following incubation in serum-free medium for 18 h, cells were treated with the test agents as specified in the text. Thereafter, cells were washed, fixed with ice-cold 4 % paraformaldehyde for 45 min, permeabilized with 0.2% Triton X-100 for 5 min. Following blockade with 3% bovine serum albumin and 1 % normal goat serum for 1 h, cells were incubated overnight at 4 °C with either rabbit polyclonal anti-phospho-cyclic AMP response element binding protein (Ser133) (pCREB) (cat no. 06-519 Upstate Biotechnology Inc., Lake Placid, NY, USA) (1:400), or rabbit monoclonal anti-phospho-S6 ribosomal protein (Ser235/236) (pS6rp) (cat. no. 4856, Cell Signaling Technology) (1:100). After washing, cells were incubated with Alexa-Fluor488-conjugated

secondary antibody (Molecular Probes/Life Technologies, Eugene, OR, USA) (1:1500) and cell nuclei were stained with 0.1 µg/ml DAPI. Cells were analyzed with an Olympus BX61 microscope equipped with a F-View II CCD-camera and mirror units for the detection of green (U-MNIBA3) and blue (U-MNUA2) fluorescence by using a 40X objective lens. Digital images were acquired using constant camera settings within each experiment and were analyzed using the program Cell P (Olympus Soft Imaging Solutions, Homburg, Germany).

For quantification, the average pixel intensity was measured within the region of the cell soma or the nucleus, as appropriate, and in an adjacent area, which was used as background value. Cells were deemed to be positive if the average pixel intensity was equal or above a threshold value corresponding to one standard deviation above the average pixel intensity of the respective control (vehicle-treated) samples. No labelling was detected in a parallel set of samples treated with preimmune IgG. Images were analyzed by an investigator unaware of the treatment.

2.6. Rho activation assay

Rho activation was measured by using the kit provided by Cell Signaling Technology (cat. no. 8820). Following treatment with the test agents, cells were washed with ice-cold PBS, and lysed by the addition of a lysis buffer supplemented with 1 mM PMSF. Cells were scraped, vortexed, and incubated on ice-bath temperature for 5 min. Thereafter, samples were centrifuged at 16,000 g for 15 min at 4 °C and the supernatants were collected and assayed for protein concentration. An aliquot containing an equal amount of protein of each sample (approximately 500 µg) was immediately mixed with glutathione S-transferase-tagged rhotekin Rho-binding domain coupled to glutathione resin in a spin cup and incubated for 1 h at 4 °C. At the end of the incubation, unbound proteins were removed by centrifugation of the spin cup at 6000 g for 30 s. Following repetitive washing

with lysis buffer, samples containing activated Rho were eluted by the addition of 2X SDS sample buffer supplemented with 200 mM dithiothreitol and heated at 100 °C for 5 min. An aliquot of the supernatant of each sample was taken prior to precipitation for determination of total Rho. Samples were analyzed by Western blot.

2.7. Morphological analysis

To examine the ability to reverse nor-adrenaline (NA)-induced astrocytes stellation, rat astrocytes were grown in six well plates in complete growth medium. Cells were then incubated for 24 h in serum-free medium, washed and exposed for 3 h to either vehicle or 10 µM NA to induce stellation. Thereafter, cells were treated for 2 h with either vehicle or the test agents as indicated in the text. The cell morphology was examined by phase-contrast light microscopy using an Olympus IX51 inverted microscope equipped with 10x Plan achromatic objective. Images were acquired in randomly selected fields by using an Olympus digital camera.

2.8. Statistical analysis

Results are reported as means ± S.D of the indicated number of independent experiments. Statistical analysis was performed by using the program Graph Pad Prism 5 (San Diego, CA, USA), which was also used to calculate EC_{50} and E_{max} values. Data are expressed as percentage or fold stimulation of control, which was included in each independent experiment. The control group was set as 100 or 1 with a variance obtained by expressing each control value as a percentage of the mean of the raw values of the control group. Statistical significance between experimental groups was assessed by either analysis of variance (ANOVA) followed by Tukey's test or Student's t test, as appropriate. A value of $P < 0.05$ was considered as the level of statistically significance.

3. Results

3.1. Stimulation of ERK1/2 by LPA in HEK-LPA$_1$, -LPA$_2$ and -LPA$_3$ cells

We firstly characterized HEK293 cells individually expressing LPA receptors with regard to their ability to respond to LPA with the phosphorylation / activation of ERK1/2, which are major effector molecules of LPA signalling in a variety of cell types. Time-course experiments showed that in HEK-LPA$_1$, -LPA$_2$ and -LPA$_3$ cells the exposure to LPA (1 µM) induced a rapid increase of dually phosphorylated ERK1/2 with a peak at 5 min, the earliest time point examined (Fig 1A-C). Thereafter, phospho-ERK1/2 levels abruptly declined, remaining higher than basal levels and showing a further rise at 30-60 min in HEK-LPA$_1$ and –LPA$_3$ cells. The stimulation of ERK1/2 was concentration-dependent with EC_{50} values of 0.53, 0.33 and 0.11 µM, and E_{max} values corresponding to 65-, 55-, and 38-fold increase of basal value in HEK-LPA$_1$, -LPA$_2$ and -LPA$_3$ cells, respectively (Fig. 1E-G and Table 1). In non-transfected HEK293 cells (HEK-WT) the exposure to LPA failed to increase phospho-ERK1/2 levels either in time-course or in concentration-response experiments (Fig.1D and H).

3.2. Differential stimulation of ERK1/2 phosphorylation in HEK-LPA$_{1-3}$ cells by tricyclic and tetracyclic antidepressants

Once it was established that transfected cells responded to LPA with a robust ERK1/2 activation, we examined the effects on this functional response of different antidepressants tested at concentrations up to 30 µM. As shown in Fig. 2, the tricyclic antidepressants amitriptyline, imipramine, clomipramine and desipramine displayed marked differences in their ability to stimulate ERK1/2 phosphorylation in HEK-LPA$_{1-3}$ cells. These drugs elicited marked stimulations in HEK-LPA$_1$ and HEK-LPA$_3$ cells, but poor responses in HEK-LPA$_2$ cells, where desipramine was without effect and the Emax values of amitriptyline,

imipramine and clomipramine corresponded to 6-11 % of that of LPA (Table 1). Conversely, the tetracyclic antidepressants mianserin and mirtazapine were effective stimulators of ERK1/2 phosphorylation at all three LPA receptors, with mianserin showing higher potency and efficacy than mirtazapine (Fig. 3 and Table 1).

The estimated EC_{50} values of tricyclic and tetracyclic antidepressants were in the low micromolar range (Table 1). At the concentration of 30 μM, amitriptyline, imipramine, desipramine, clomipramine and mianserin failed to induce a significant increase of phospho-ERK1/2 levels in HEK-WT cells (Supplementary Fig. 1).

3.3. Potentiation of LPA-induced ERK1/2 activation by amitriptyline and mianserin

We next examined the effects of the combined treatment with antidepressants and LPA on the activation of ERK1/2. HEK-LPA_{1-3} cells were exposed for 2 min to a low concentration of either amitriptyline (1 μM) or mianserin (0.5 μM) and then treated for 5 min with a threshold concentration of LPA (10 nM). Both antidepressants had no effect *per se* but significantly potentiated ERK1/2 phosphorylation induced by LPA in HEK-LPA_1, -LPA_2 and LPA_3 cells (Fig. 4). A similar potentiation of the LPA response by the two antidepressants was observed in HT22 hippocampal cells and CHO-K1 fibroblasts, which express LPA receptors under native conditions (Fig. 4). Conversely, in HEK-LPA_1 cells both amitriptyline and mianserin had no effect on ERK1/2 phosphorylation induced by 10 pg/ml FGF-2 (Supplementary Figure 2).

3.4 Enhancement of LPA-induced phosphorylation of CREB and S6 ribosomal protein by amitriptyline and mianserin in HEK-LPA_1 cells.

To investigate whether the potentiation of LPA-induced ERK1/2 activation elicited by amitriptyline and mianserin translated into an altered regulation of downstream effector

molecules we examined the expression levels of phospho-CREB and phospho-S6 ribosomal protein, which are known to be upregulated by ERK1/2 signalling. Immunofluorescence analysis of HEK-LPA_1 cells indicated that phospho-S6 ribosomal protein immunoreactivity showed a cytoplasmic localization, being absent in the nuclear region, whereas phospho-CREB immunoreactivity had a nuclear localization, as indicated by the overlapping with DAPI staining (Fig. 5). Cell treatment with either amitriptyline (1 uM) or mianserin (0.5 μM) had no effect on the expression levels of the two phosphorylated proteins but significantly enhanced the LPA-induced increase of the percentage of cells positive for either phospho-S6 ribosomal protein or phospho-CREB immunoreactivity (Fig. 5).

3.5. Evidence that $G_{q/11}$ and $G_{i/o}$ mediate LPA-induced AMPK and ERK1/2 phosphorylation, respectively.

The coupling of LPA receptors to $G_{q/11}$ is known to stimulate phospholipase C causing the formation of inositol trisphosphate, which rapidly triggers the mobilization of Ca^{2+} from intracellular stores. In several cell types, the increased intracellular Ca^{2+} has been shown to promote the Ca^{2+}/calmodulin-dependent protein kinase kinase-β-mediated phosphorylation of the α subunit of AMPK (AMPKα) at Thr172 and the consequent activation of the kinase (Hawley et al., 2005; Woods et al., 2005), which functions as a pivotal regulator of cellular energy homeostasis (Hardie et al., 2012). Accordingly, a brief exposure (5 min) of HEK-LPA_1 cells to the Ca^{2+} ionophore ionomycin (100 nM) induced a marked increase in the steady state levels of phospho-AMPKα, indicating that elevation of intracellular Ca^{2+} regulates AMPK in these cells. (Supplementary Fig. 3). Similarly, to ionomycin, acute treatment of HEK-LPA_1 cells with LPA (1 μM) induced a significant increase of phospho-AMPKα levels and this effect was blocked by cell pre-treatment with

the $G\alpha_{q/11}$ antagonist YM-254890 (10 µM) (Takasaki et al., 2004) (Fig. 6). Conversely, cell pre-treatment with PTX (100 nM), which uncouples $G_{i/o}$ from receptors, did not prevent LPA stimulation of AMPK (Fig. 6) but abrogated the activation of ERK1/2 by the phospholipid (Supplementary Fig.4).

3.6. Effects of amitriptyline and mianserin on LPA-induced AMPK phosphorylation in HEK-LPA_{1-3} cells

We then investigated the effects of either amitriptyline (1 µM) or mianserin (0.5 µM) on the stimulation of AMPKα phosphorylation by LPA (1 µM) in HEK-LPA_{1-3} cells. Both antidepressants failed to affect phospho-AMPKα levels but potentiated the LPA stimulation in HEK-LPA_1 and -LPA_3 cells (Fig. 7). In contrast, no significant enhancement of LPA effect by either amitriptyline or mianserin was observed in HEK-LPA_2 cells (Fig. 7).

3.7. Amitriptyline and mianserin curtail LPA-induced Rho activation in HEK-LPA_1 and -LPA_2 cells

Rho proteins are a family of small G proteins that are activated by LPA receptors through the coupling to $G_{12/13}$ (Kihara et al., 2014; Stoddard and Chun, 2015). The exposure to either amitriptyline (1 µM) or mianserin (0.5 µM) had no significant effect on basal levels of activated Rho in HEK-LPA_{1-3} cells (Fig. 8). LPA (1 µM) increased the levels of activated Rho in HEK-LPA_1 and -LPA_2 but not -LPA_3 cells (Fig.8). When combined with LPA, both amitriptyline and mianserin caused a significant inhibition of the phospholipid stimulation in HEK-LPA_1 and -LPA_2 cells and did not modify the response of HEK-LPA_3 cells to LPA (Fig. 8).

3.8 Mianserin fails to mimic the LPA reversal of noradrenaline-induced astrocyte stellation.

Treatment of cultured astrocytes with cyclic AMP-stimulating agents or cyclic AMP analogs in serum-free conditions is known to induce profound structural changes, such as retraction of cytoplasm toward the perinuclear region, rounding of the soma and the formation of thin processes, leading to the acquisition of a stellate morphology (Shapiro, 1973; Tas and Koschel, 1990). The addition of LPA has been shown to reverse astrocyte stellation through the activation of RhoA and the consequent assembly of stress fibers and focal adhesions (Suidan et al., 1997; Ramakers and Moolenaar, 1998). We therefore examined whether the exposure to mianserin was capable of mimicking LPA-induced reversal of astrocyte stellation. As shown in Fig. 9, treatment of rat astrocytes with the adrenergic agonist noradrenaline (10 μM) induced the appearance of stellation in a large number of astrocytes. This morphological change was almost completely reversed by the subsequent incubation with LPA (10 μM). In contrast, the addition of mianserin (10 μM) had no significant effect on noradrenaline-induced stellation.

4. Discussion

An important outcome of the present study is the demonstration that widely used tricyclic and tetracyclic antidepressants can target not only LPA_1, as previously reported, but also LPA_2 and LPA_3. The study also reveals marked differences in the intrinsic activities of the drugs at each EDG receptor subtype and the manner they modulate LPA-induced activation of distinct signalling pathways. Thus, the analysis of ERK1/2 activation indicated that tricyclic antidepressants amitriptyline, clomipramine and desipramine behaved as efficacious agonists at LPA_1 and LPA_3 but displayed poor activity at LPA_2. Moreover, as compared to imipramine, the demethylated derivative desipramine showed a much lower intrinsic activity at LPA_1 and LPA_3 and no effect at LPA_2. These results indicate that minor

changes in the chemical structure can result in marked differences in the efficacy of antidepressants as agonists of LPA_{1-3} receptors coupled to ERK1/2 stimulation. This concept is further supported by the data obtained examining mianserin and mirtazapine. Unlike the tricyclic agents, these antidepressants, which possess a tetracyclic piperazinoazepine structure, were capable of stimulating ERK1/2 phosphorylation at LPA_1, LPA_2 and LPA_3. However, mirtazapine, which differs from mianserin only for having an isosteric replacement of CH by N in the aromatic A ring, displayed two/three-fold lower potencies and efficacies than mianserin.

Low concentrations of either amitriptyline or mianserin, which per se were unable to activate ERK1/2, potentiated the stimulatory effect of a threshold concentration of LPA in HEK-LPA_1, -LPA_2 and -LPA_3 cells. This synergistic interaction was also observed in CHO-K1 fibroblasts and HT22 hippocampal cells, which express LPA receptors under native conditions, thus ruling out a possible dependence on receptor over-expression. Moreover, at the same concentration the two antidepressants failed to affect ERK1/2 stimulation by FGF-2 in HEK-LPA_1 cells, implying that the synergism with LPA has some degree of selectivity. On the other hand, in these cells immunofluorescence analysis showed that LPA-induced increase in phospho-CREB and phospho-S6rp expression was significantly enhanced by exposure to a low concentration of either amitriptyline or mianserin. Previous studies have demonstrated that ERK1/2 plays a pivotal role in the coupling of LPA receptor activation to CREB phosphorylation (Lee et al., 2003; Olianas et al., 2015). ERK1/2 kinases can induce CREB and S6rp phosphorylation through the activation of p90 S6 ribosomal kinases (RSKs) (Roux and Blenis, 2004; Roux et al., 2007). Thus, the enhancement of LPA-induced phosphorylation of CREB and S6rp likely results from the synergistic activation of ERK1/2. Interestingly, several studies have shown that the upregulation of phospho-CREB and phospho-S6rp plays a role in the control of synaptic

plasticity (Benito and Barco 2010; Biever et al. 2015). In addition, CREB activity has been involved in the regulation of emotional behaviour (Blendy, 2006; Ren X. et al., 2014). Collectively, these findings suggest that a synergistic interaction between antidepressants and LPA affects critical components of the intracellular signalling cascades and neurochemical events potentially linked to cognitive and affective functions.

LPA enhanced the activating phosphorylation of AMPKα in HEK-LPA_1, -LPA_2, and -LPA_3 cells. The LPA stimulation was inhibited by YM-254890 and, unlike ERK1/2 activation, largely insensitive to PTX, implying the mediation by $G_{q/11}$ rather than $G_{i/o}$. In the brain, activated AMPK is known to play a critical role in the maintenance of cellular energy homeostasis and has been shown to exert neuroprotective effects in response to reduced energy supply (Ronnet et al., 2009). Moreover, there is evidence that in animal models of depression AMPK is inactivated (Zhu et al., 2014) and its stimulation can produce antidepressant-like behaviour and hippocampal neurogenesis (Odaira et al., 2019). Thus, it was of interest to examine whether the antidepressants could also affect the AMPK response to LPA at each receptor subtype. Amitriptyline and mianserin were found to potentiate LPA-induced AMPKα phosphorylation in LPA_1- and LPA_3-expressing cells, indicating that the synergistic interaction also occurred at a LPA signalling pathway regulated by $G_{q/11}$. On the other hand, both antidepressants had no effect on LPA-induced stimulation of AMPK in HEK-LPA_2 cells, showing a lack of sensitivity of the LPA_2-AMPK coupling mechanism to the facilitatory action of the drugs. It is noteworthy that the LPA_2 receptor differs from the other LPA receptors in having a unique carboxyl-terminal tail, which binds several interacting proteins containing PDZ and zinc finger domains. These proteins have been shown to regulate distinct LPA_2 receptor functions, including the coupling to PLC-β and calcium mobilization (Lin and Lai, 2008; Ren A. et al., 2014). Additional studies are required to investigate whether the failure of antidepressants to

potentiate AMPK activation induced by LPA in LPA_2-expressing cells is related to the action of these receptor interacting proteins.

The stimulation of the $G_{12/13}$-RhoA signalling pathway has been implicated in several biological responses triggered by LPA receptors, including induction of cell migration (Manning et al., 2000; Bian et al., 2006), regulation of cell shape (Ridley and Hall, 1992; Tigyi et al., 1996) and initiation of neuropathic pain (Inoue et al., 2004). We found that both amitriptyline and mianserin inhibited LPA-induced Rho activation in HEK-LPA_1 and HEK-LPA_2 cells. In HEK-LPA_3 cells either LPA or antidepressants failed to induce significant changes in the levels of activated Rho. The lack of effect by LPA is in line with the previous observation that in LPA_3-transfected B103 cells LPA failed to induce cell rounding, a Rho dependent response (Ishi et al., 2000). Moreover, in cultured rat astrocytes mianserin, examined at a concentration effective in stimulating ERK1/2 through LPA_1 (Olianas et al., 2016), did not mimic the reversal action of LPA on noradrenaline-induced stellation. These results suggest that the antidepressants are not only unable to activate Rho per se, but also exert a negative effect on the coupling of LPA_1 and LPA_2 to Rho.

5. Conclusions

The ability of tricyclic and tetracyclic antidepressants to act on LPA_2 and LPA_3 receptors may extend their spectrum of action on LPA signalling beyond that mediated by the LPA_1 subtype. By using a receptor / β-arrestin interaction assay, we previously reported that both amitriptyline and mianserin failed to stimulate β-arrestin recruitment to LPA_2 and LPA_3 receptors individually expressed in CHO-K1 cells (Olianas et al., 2015). Taken together with the present results, this observation raises the possibility, which requires further investigation, that the two antidepressants favour the coupling of LPA receptor to G

proteins over β-arrestin. Moreover, the present study indicate that these drugs can differentially modulate signalling pathways activated by LPA via EDG receptors, amplifying the responses mediated by $G_{i/o}$ and $G_{q/11}$ and curtailing those through $G_{12/13}$. In future studies it will be important to investigate whether and how this modulatory action contributes to the therapeutic and/or adverse effects of these drugs.

Declaration of competing interest

The authors declare no conflict of interest.

Acknowledgements

This work was partially supported by University of Cagliari, Italy (FIR 2019).

References

Banks, D.B., Chan, G.N.Y., Evans, R.A., Miller, D.S., Cannon, R.E., 2018. Lysophosphatidic acid and amitriptyline signal through LPA1R to reduce P-glycoprotein transport at the blood-brain barrier. J. Cereb. Blood Flow Metab. 38, 857-868. doi: 10.1177/0271678X17705786.

Benito, E., Barco, A., 2010. CREB's control of intrinsic and synaptic plasticity: implications for CREB-dependent memory models. Trends Neurosci. 33, 230-240. doi: 10.1016/j.tins.2010.02.001.

Bian, D., Mahanivong, C., Yu, J., Frisch, S.M., Pan, Z.K., Ye, R.D., Huang, S., 2006. The $G_{12/13}$-RhoA signaling pathway contributes to efficient lysophosphatidic acid-stimulated cell migration. Oncogene 25, 2234-2244. doi: 10.1038/sj.one.1209261.

Biever, A., Valjent, E., Pulghermanal, E., 2015. Ribosomal protein S6 phosphorylation in the nervous system: from regulation to function. Front. Mol. Neurosci. 8: 75. doi: 10.3389/fnmol.2015.00075.

Blendy, J.A., 2006. The role of CREB in depression and antidepressant treatment. Biol. Psychiatry 59, 1144-1150. doi: 10.1016/j.biopsych.2005.11.003.

Geraldo, L.H.M., Spohr, T.C.L., do Amaral, R.F., Carvalho da Fonseca, A.C., Garcia, C., de Almeida Mendes, F., Freitas, C., dosSantos, M.F., Souza Lima, F.R., 2021. Role of lysophosphatidic acid and its receptors in health and disease: novel therapeutic strategies.

Signal Trasduct. Target Ther. 6, 45. doi: 10.1038/s41392-020-00367-5.

Hardie, D.G., Ross, F.A., Hawley, S.A., 2012. AMPK: a nutrient and energy sensor that maintains energy homeostasis. Nat. Rev. Mol. Cell Biol. 13, 251-262. doi: 10.1038/nrm3311.

Hawley, S.A., Pan, D.A., Mustard, K.J., Ross, L., Bain, J., Edelman, A.M., Frenguelli, B.G., Hardie, D.G., 2005. Calmodulin-dependent protein kinase kinase-beta is an alternative upstream kinase for AMP-activated protein kinase. Cell Metab. 2, 9-19. doi: 10.1016/j.cmet.2005.05.009.

Inoue, M., Rashid, M.H., Fujita, R., Contos, J.J.A., Chun, J., Ueda, H., 2004. Initiation of neuropathic pain requires lysophosphatidic acid receptor signaling. Nat. Med. 10, 712-718. doi: 10.1038/nm1060.

Ishii, I., Contos, J.J.A., Fukushima, N., Chun, J., 2000. Functional comparisons of the lysophosphatidic acid receptors, LP_{A1}/VZG-1/EDG-2, LP_{A2}/EDG-4, and LP_{A3}/EDG-7 in neuronal cell lines using a retrovirus expression system. Mol. Pharmacol. 58, 895-902. doi:10.1124/mol.58.5.895.

Kajitani, N., Miyano, K., Okada-Tsuchioka, M., Abe, H., Itagaki, K., Hisaoka-Nakashima, K., Morioka, N., Uezono, Y., Takebayashi, M., 2016. Identification of lysophosphatidic acid receptor 1 in astroglial cells as a target for glial cell line-derived neurotrophic factor expression induced by antidepressants. J. Biol. Chem. 291, 27364-27370. doi: 10.1074/jbc.M116.753871.

Kihara, Y., Maceyka, M., Spiegel, S., Chun, J., 2014. Lysophospholipid receptor nomenclature review: IUPHAR Review 8. Br. J. Pharmacol. 171, 3575-3594. doi: 10.1111/bph.12678.

Lee, C.-W., Nam, J.-S., Park, Y.-K., Choi, H.-K., Lee, J.-H., Kim, N.-H., Cho, J., Song, D.-K., Suh, H.-W., Lee, J., Kim, W.-H., Huh, S.-O., 2003. Lysophosphatidic acid stimulates CREB through mitogen- and stress-activated protein kinase-1. Biochem. Biophys. Res. Commun. 305, 455-461. doi: 10.1016/S0006-291X(03)00790-3.

Lin, F.-T., Lai, Y.-J., 2008. Regulation of the LPA_2 receptor signaling through the carboxyl-terminal tail-mediated protein-protein interactions. Biochim. Biophys. Acta 178, 558-562. doi: 10.1016/j.bbalip.2008.04.013.

Manning, T.J., Parker, J.C., Sontheimer, H., 2000. Role of lysophosphatidic acid and Rho in glioma cell motility. Cell Motil. Cytoskeleton 45, 185-199. doi:10.1002/(SICI)1097-0169(200003)45:3<185::AID-CM2>3.0.CO;2-G.

Odaira, T., Nakagawasai, O., Takahashi, K., Nemoto, W., Sakuma, W., Lin, J.-R., Tan-No, K., 2019. Mechanisms underpinning AMP-activated protein kinase-related effects on behavior and hippocampal neurogenesis in an animal model of depression. Neuropharmacology 150, 121-133. doi: 10.1016/j.neuropharm.2019.03.026.

Olianas, M.C., Dedoni, S., Onali P., 2015. Antidepressants activate the lysophosphatidic acid receptor LPA_1 to induce insulin-like growth factor-1 receptor transactivation ,

stimulation of ERK1/2 signaling and cell proliferation in CHO-K1 fibroblasts. Biochem. Pharmacol. 95, 311-323. doi: 10.1016/j.bcp.2015.04.002.

Olianas, M.C., Dedoni, S., Onali P., 2016. LPA_1 mediates antidepressant-induced ERK1/2 signaling and protection from oxidative stress in glial cells. J. Pharmacol. Exp. Ther. 359, 340-353. doi: 10.1124/jpet.116.236455.

Olianas, M.C., Dedoni, S., Onali P., 2017. LPA_1 is a key mediator of intracellular signalling and neuroprotection triggered by tetracyclic antidepressants in hippocampal neurons. J. Neurochem. 143, 183-197. doi: 10.1111/jnc.14150.

Olianas, M.C., Dedoni, S., Onali P., 2019. Inhibition of TNF-α-induced neuronal apoptosis by antidepressants acting through the lysophosphatidic acid receptor LPA_1. Apoptosis 24, 478-498. doi: 10.1007/s10495-019-01530-2.

Olianas, M.C., Dedoni, S., Onali P., 2020. Antidepressants induce profibrotic responses via the lysophosphatidic acid receptor LPA_1. Eur. J. Pharmacol. 873, 172963. doi: 10.1016/j.ejphar.2020.172963.

Ramakers, G.J.A., Moolenaar, W.H., 1998. Regulation of astrocyte morphology by RhoA and lysophosphatidic acid. Exp. Cell Res. 245, 252-262. doi: 10.1006/excr.1998.4224.

Ren, A., Moon, C., Zhang, W., Sinha, C., Yarlagadda, S., Arora, K., Wang, X., Yue, J., Perthasarathi, K., Heil-Chapdelaine, R., Tigyi, G., Naren, A.P., 2014. Asymmetrical macromolecular complex formation of lysophosphatidic acid receptor 2 (LPA_2) mediates

gradient sensing in fibroblasts. J. Biol. Chem. 289, 35757-35769. doi: 10.1074/jbc.M114.595512.

Ren, X., Rizavi, H.S., Khan, M.A., Bhaumik, R., Dwivedi, Y., Pandey, G.N., 2014. Alteration of cyclic-AMP response element binding protein in the post-mortem brain of subjects with bipolar disorder and schizophrenia. J. Affect. Disord. 152-154, 326-333. doi: 10.1016/j.jad.2013.09.033.

Ridley, A.J, Hall, A., 1992. The small GTP binding protein rho regulates the assembly of focal adhesions and actin stress fibers in response to growth factors. Cell 70, 380-399. doi: 10.1016/0092-8674(92)90163-7.

Ronnett, G.V. Ramamurthy, S., Kleman, A.M., Landree, L.E., Aja, S., 2009. AMPK in the brain: its roles in energy balance and neuroprotection. J. Neurochem. 109 (Suppl.1), 17-23. doi: 10.1111/j.1471-4159.2009.05916.x.

Roux, P.P., Blenis, J., 2004. ERK and p38 MAPK-activated protein kinases: a family of protein kinases with diverse biological functions. Microbiol. Mol. Biol. Rev. 68, 320-344. doi: 10.1128/MMBR.68.2.320-344.2004.

Roux, P.P., Shahbazian, D., Vu, H., Holz, M.K., Cohen, M.S., Taunton, J., Sonenberg, N., Blenis, J., 2007. RAS-ERK signaling promotes site-specific ribosomal protein S6 phosphorylation via RSK and stimulates cap-dependent translation. J. Biol. Chem. 282, 14056-14064. doi: 10.1074/jbc.M700906200.

Shapiro, D.L., 1973. Morphological and biochemical alterations in foetal rat brain cells cultured in the presence of monobutyryl cyclic AMP. Nature 241, 203-204. doi: 10.1038/241203a.0.

Schober, A., Siess, W., 2012. Lysophosphatidic acid in atherosclerotic diseases. Br. J. Pharmacol. 167, 465-482. doi: 10.1111/j.1476-5381.2012.02021.x.

Solis, K.H., Romero-Avila, M.T., Guzman-Silva, A., Garcia-Sainz, J.A., 2021. The LPA_3 receptor: regulation and activation of signaling pathways. Int. J. Mol. Sci. 22, 6704. doi: 10.3390/ijms22136704.

Stoddard, N.C., Chun, J., 2015. Promising pharmacological directions in the world of lysophosphatidic acid signaling. Biomol. Ther. 23, 1-11. doi: 10.4062/biomolther.2014.109.

Suidan, H.S., Nobes, C.D., Hall, A., Monard, D., 1997. Astrocyte spreading in response to thrombin and lysophosphatidic acid is dependent on the Rho GTPase. Glia 21, 244-252. doi: 10.1002/(sici)1098-1136(199710)21:2<244::aid-glia7>3.0.co;2-6.

Takasaki, J., Saito, T., Taniguchi, M., Kawasaki, T., Moritani, Y., Hayashi, K., Kobori, M., 2004. A novel $G\alpha_{q/11}$-selective inhibitor. J. Biol. Chem. 279, 47438-47445. doi: 10.1074/jbc.M408846200.

Tas, P.W., Koschel, K., 1990. Thrombin reverts the β-adrenergic agonist-induced morphological response in rat glioma C6 cells. Exp. Cell Res. 189, 22-27. doi: 10.1016/0014-4827(90)90251-5.

Tigyi, G., 2010. Aiming drug discovery at lysophosphatidic acid targets. Br. J. Pharmacol. 161, 241-270. doi: 10.1111/j.1476-5381.2010.00815.x.

Tigyi, G., Fisher, D.J., Sebok, A., Marshall, F., Dyer, D.L., Miledi, R., 1996. Lysophosphatidic acid-induced neurite retraction in PC12 cells: neurite-protective effects of cyclic AMP signaling. J. Neurochem. 66, 549-558. doi: 10.1046/j.1471-4159.1996.66020549.x.

Woods, A., Dickerson, K., Heath, R., Hong, S.P., Momcilovic, M., Johnstone, S.R., Carlson, M., Carling, D., 2005. Ca^{2+}/calmodulin-dependent protein kinase kinase-β acts upstream of AMP-activated protein kinase in mammalian cells. Cell Metab. 2, 21-33. doi: 10.1016/j.cmet.2005.06.005.

Yung, Y.C., Stoddard, N.C., Chun, J., 2014. LPA receptor signaling, pharmacology, physiology, and pathophysiology. J. Lipid Res. 55, 1192-1214. doi: 10.1194/jlr.R046458.

Yung, Y.C., Stoddard, N.C., Mirendil, H. Chun, J., 2015. Lysophosphatidic acid signaling in the nervous system. Neuron 85, 669-682. doi: 10.1016/j.neuron.2015.01.009.

Zhu, S., Wang, J., Zhang, Y., Li, V., Kong, J., He, J., Li, X.-M., 2014. Unpredictable chronic mild stress induces anxiety and depression-like behaviors and inactivates AMP-activated protein kinase in mice. Brain Res. 1576, 81-90. doi: 10.1016/j.brainres.2014.06.002.

Table 1

Properties of antidepressants in activating ERK1/2 in HEK-LPA_1, -LPA_2, and –LPA_3 cells

	HEK-LPA_1			HEK-LPA_2			HEK-LPA_3		
	EC_{50} (μM)	E_{max}[a]	rel.E_{max}[b]	EC_{50} (μM)	E_{max}[a]	rel.E_{max}	EC_{50} (μM)	E_{max}[a]	rel.E_{max}[b]
LPA	0.53 ± 0.06	65 ± 7	100	0.33 ± 0.02	55 ± 5	100	0.11 ± 0.01	38 ± 6	100
Amitriptyline	6.70 ± 0.2	19 ± 2	29	N.D.	3.5 ± 0.3	6	10.3 ± 0.8	27 ± 2	72
Clomipramine	13.2 ± 0.4	39 ± 3	60	N.D.	6.3 ± 0.8	11	3.3 ± 0.4	28 ± 4	74
Imipramine	13.7 ± 0.3	19 ± 1	29	N.D.	5.5 ± 0.6	10	14.7 ± 0.5	21 ± 1	55
Desipramine	7.5 ± 0.4	10 ± 1	15	N.D.	N.D.	N.D.	11.8 ± 0.3	11 ± 1	29
Mianserin	4.4 ± 0.2	52 ± 3	80	4.1 ± 0.1	51 ± 4	93	3.2 ± 0.2	33 ± 2	87
Mirtazapine	10.9 ± 0.6	24 ± 2	37	18.1 ± 0.4	15 ± 3	27	14.8 ± 0.4	20 ± 2	53

[a] E_{max}= fold of stimulation; [b] rel.E_{max} = (E_{max} test agent / E_{max} LPA) x 100. Values are the mean ± S.D. of three (LPA) and four (antidepressants) independent experiments. N.D., not determined.

Figure legends

Fig.1. Stimulation of ERK1/2 phosphorylation by LPA in HEK-LPA_1, -LPA_2, - LPA_3, and -WT cells. A-D. Cells were serum starved for 24 h and then incubated for the indicated periods of time with 1 μM LPA The levels of phospho-ERK1/2 (pERK1/2) and total ERK1/2 were measured in cell extracts by Western blot. Densitometric ratios are expressed as fold of stimulation with respect to 0 time (vehicle-treated cells). E-H: Cells were incubated for 5 min with either vehicle or the indicated concentrations of LPA. Values are the mean ± S.D. of three separate experiments. * $P < 0.05$, ** $P < 0.01$, *** $P < 0.001$ vs vehicle by ANOVA followed by Tukey's test .

Fig. 2. Concentration-dependent stimulation of ERK1/2 phosphorylation by tricyclic antidepressants in HEK-LPA_1, -LPA_2, and -LPA_3 cells. Serum-starved cells were incubated for 5 min with either vehicle or the indicated concentrations of amitriptyline, clomipramine, imipramine and desipramine. Values are expressed as fold stimulation and are the mean ± S.D. of four independent experiments. * $P < 0.05$, ** $P < 0.01$, *** $P < 0.001$ vs vehicle by ANOVA followed by Tukey's test.

Fig. 3. Concentration-dependent stimulation of ERK1/2 phosphorylation by tetracyclic antidepressants in HEK-LPA_1, -LPA_2, and -LPA_3 cells. Serum-starved cells were incubated for 5 min with either vehicle or the indicated concentrations of mianserin and mirtazapine Values are expressed as fold stimulation and are the mean ± S.D. of four independent experiments. * $P < 0.05$, *** $P < 0.001$ vs vehicle by ANOVA followed by Tukey's test.

Fig. 4. Potentiation of LPA-stimulated ERK1/2 phosphorylation by amitriptyline and mianserin. Serum-starved HEK-LPA_1, -LPA_2, LPA_3, HT22, and CHO-K1 cells were

incubated for 2 min with either vehicle, amitriptyline (Ami) (1 µM) or mianserin (Mians) (0.5 µM), and then exposed for 5 min to either vehicle or LPA (10 nM) for 5 min. Cell extracts were analyzed for phosphorylated and total ERK1/2 by Western blot. Densitometric ratios are expressed as percent of control (vehicle) and are the mean ± S.D. of four experiments. * $P < 0.05$, *** $P < 0.001$ vs vehicle, $^{\#\#}$ $P < 0.01$, $^{\#\#\#}$ $P < 0.001$ vs LPA alone by ANOVA followed by Tukey's test.

Fig. 5. Immunofluorescence analysis of phospho-S6 ribosomal protein (pS6rp) and phospho-CREB (pCREB) in HEK-LPA_1 cells. Serum-starved cells were exposed for 2 min with either vehicle, amitriptyline (Ami) (1 µM) or mianserin (Mians) (0.5 µM) and then incubated for 30 min with either vehicle or LPA (10 nM). Cells were analyzed for pS6rp and pCREB immunoreactivity (green color) by fluorescence microscopy. Nuclei were stained with DAPI (blue color). The number of positive cells was determined in each experimental group and expressed as percent of total cells. Values are the mean ± S.D. of five separate experiments. Bar = 100 µm. * $P < 0.05$, ** $P < 0.01$ vs vehicle, $^{\#}$ $P < 0.05$, $^{\#\#}$ $P < 0.01$, $^{\#\#\#}$ $P < 0.001$ vs LPA alone by ANOVA followed by Tukey's test.

Fig. 6. Inhibition of LPA-induced AMPKα phosphorylation by the $G\alpha_{q/11}$ antagonist YM-254890 but not PTX. A: HEK-LPA_1 cells were incubated for 20 min with either vehicle or YM-254890 (YM) (10 µM) and then exposed to either vehicle or LPA (1 µM) for 5 min. B: Cells were preincubated for 24 h with either vehicle or PTX (100 ng/ml). Thereafter, the cells were washed and incubated in serum-free medium with either vehicle or LPA (1 µM). Cell extracts were analyzed for phospho-AMPKα (pAMPK) and total AMPKα levels by Western blot. Densitometric ratios are expressed as percent of control (vehicle) and are

the mean ± S.D. of three experiments. ** $P < 0.01$ vs vehicle, $^{\#}$ $P < 0.01$ vs LPA alone, ^{ns} not significantly different by ANOVA followed by Tukey's test.

Fig. 7. Effects of amitriptyline and mianserin on LPA-induced AMPKα phosphorylation in HEK-LPA_1, -LPA_2, and –LPA_3 cells. Cells were incubated for 2 min with either vehicle, amitriptyline (Ami) (1 µM) or mianserin (Mians) (0.5 µM) and then exposed for 5 min to either vehicle or LPA (1 µM). Densitometric ratios are expressed as percent of control (vehicle) and are the mean ± S.D. of four experiments. * $P < 0.05$ vs vehicle, $^{\#}$ $P < 0.05$, $^{\#\#}$ $P < 0.01$ vs LPA alone, ^{ns} not significantly different by ANOVA followed by Tukey's test.

Fig. 8. Inhibition of LPA-induced Rho activation by amitriptyline and mianserin. HEK-LPA_1, -LPA_2, and –LPA_3 cells were incubated for 2 min with either vehicle, amitriptyline (Ami) (1 µM) or mianserin (Mians) (0.5 µM) and then exposed for 5 min to either vehicle or LPA (1 µM). Cell extracts were then analyzed for active and total Rho (input) by Western blot. Densitometric ratios are expressed as percent of control (vehicle) and are the mean ± S.D. of three experiments. * $P < 0.05$, *** $P < 0.001$ vs vehicle, $^{\#}$ $P < 0.05$, $^{\#\#}$ $P < 0.01$ vs LPA alone by ANOVA followed by Tukey's test.

Fig. 9. Mianserin fails to mimic LPA-induced reversal of astrocyte stellation. Cultured rat astrocytes were incubated in serum-free medium with either vehicle or noradrenaline (NA) (10 µM) for 3 h and then exposed for 2 h to either vehicle, LPA (10 µM) or mianserin (Mians) (10 µM). Phase contrast images are representative of three separate experiments. Bar = 100 µm.

Declaration of interests

☒The authors declare that they have no known competing financial interests or personal relationships that could have appeared to influence the work reported in this paper.

☐The authors declare the following financial interests/personal relationships which may be considered as potential competing interests:

Figure 1

Click here to access/download;Figure;Fig 1.tif

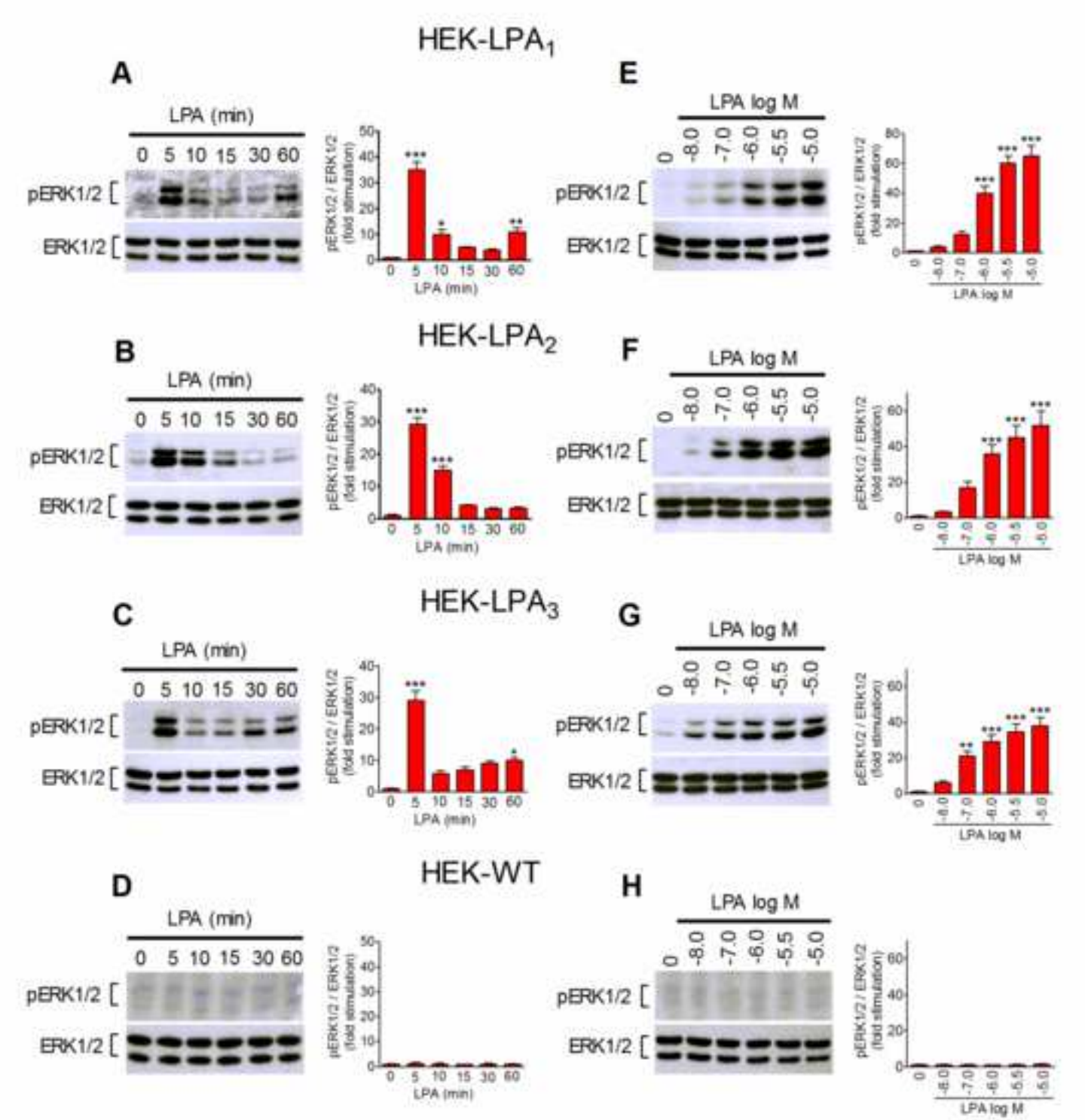

Fig. 1

Figure 2

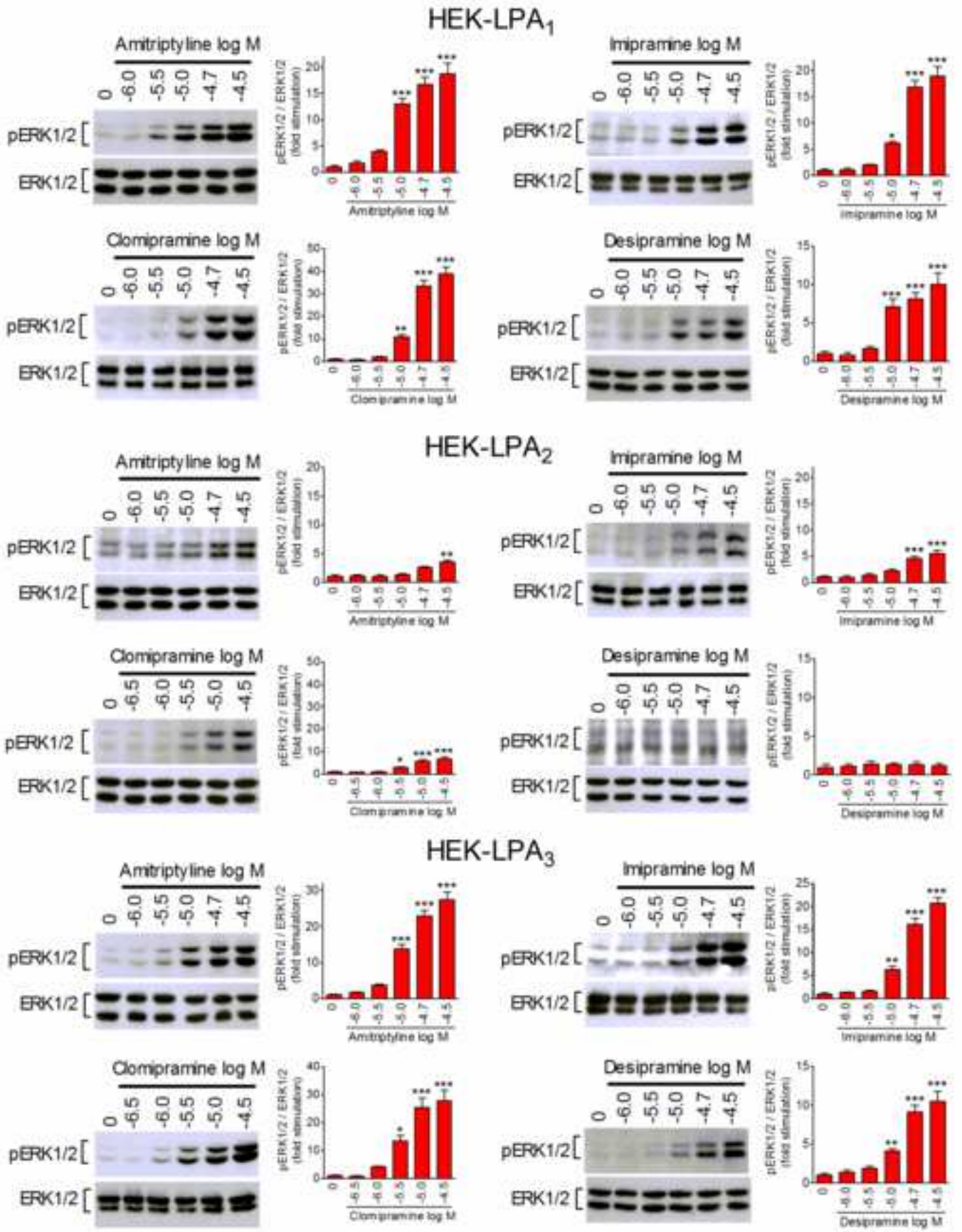

Fig. 2

Figure 3

Click here to access/download;Figure;Fig 3.tif

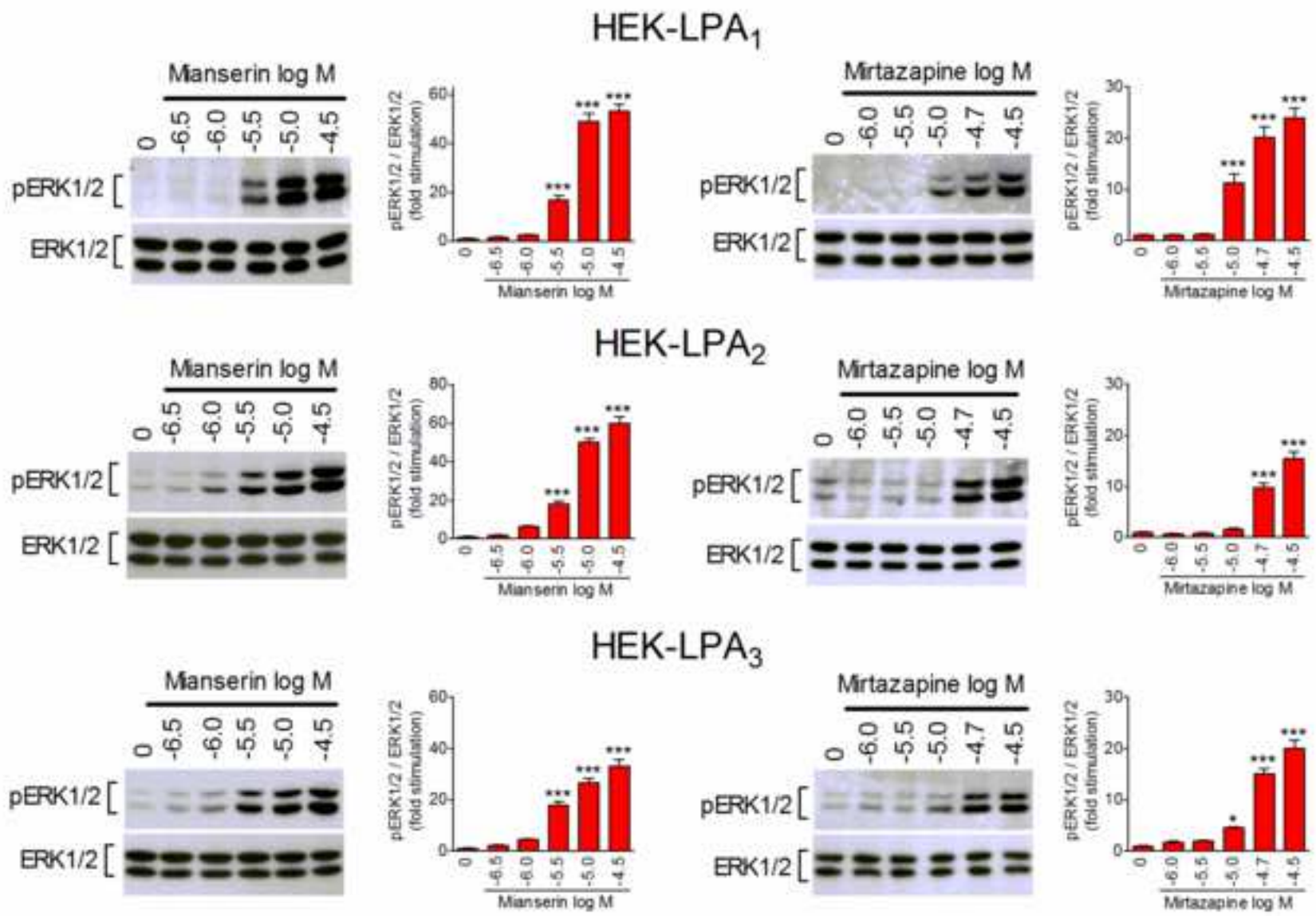

Fig. 3

Figure 4

Click here to access/download;Figure;Fig 4.tif

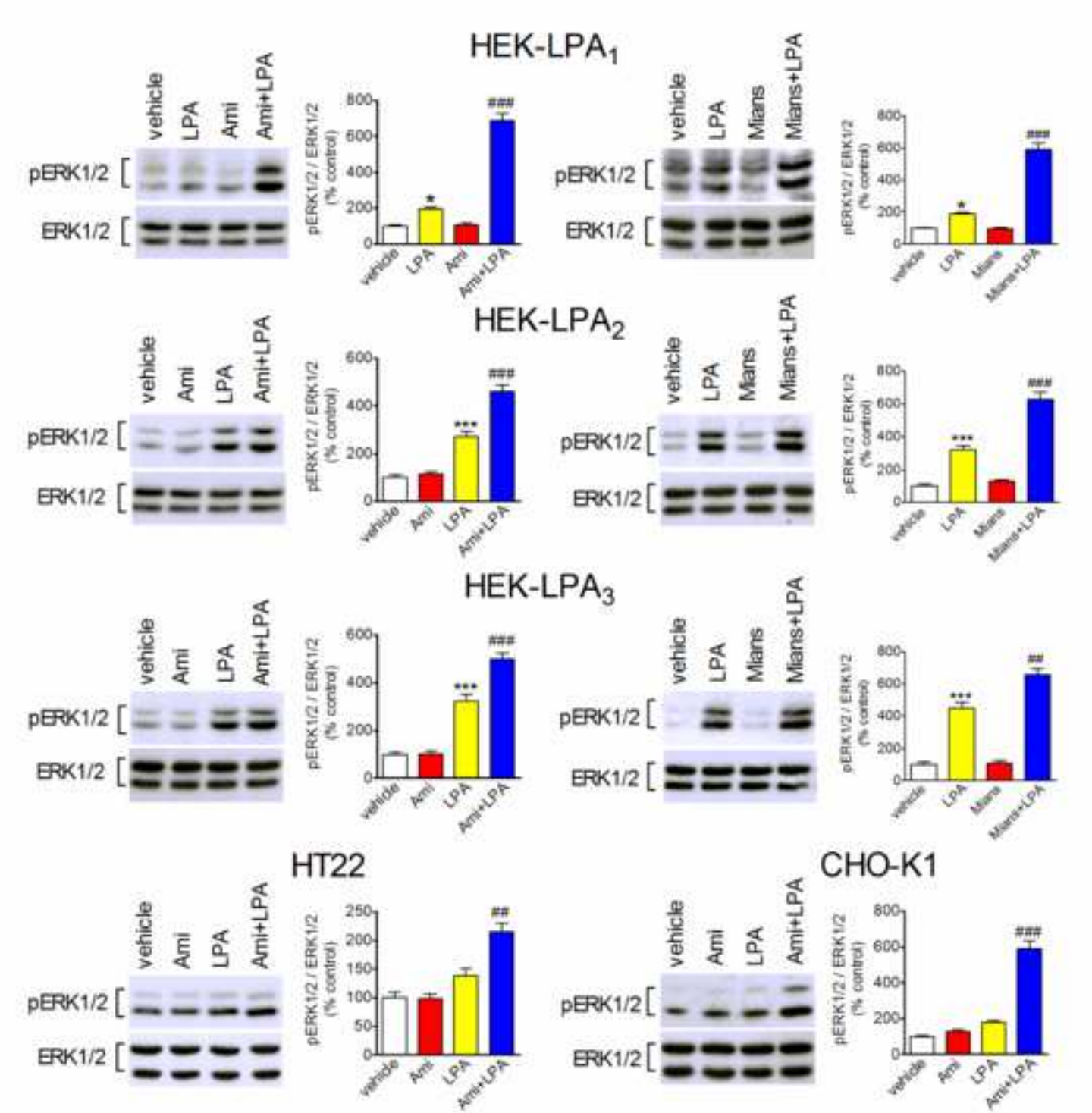

Fig. 4

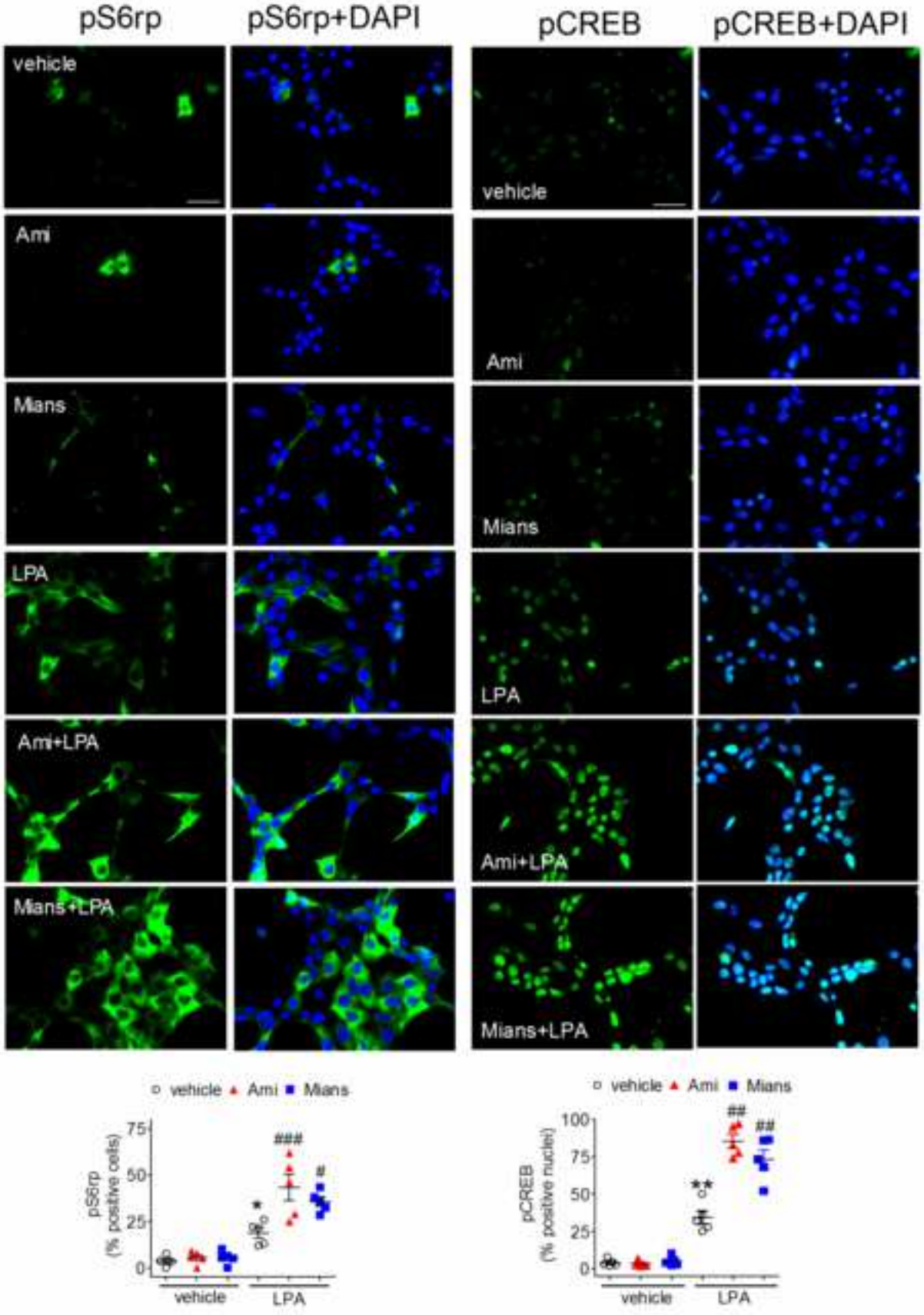

Fig. 5

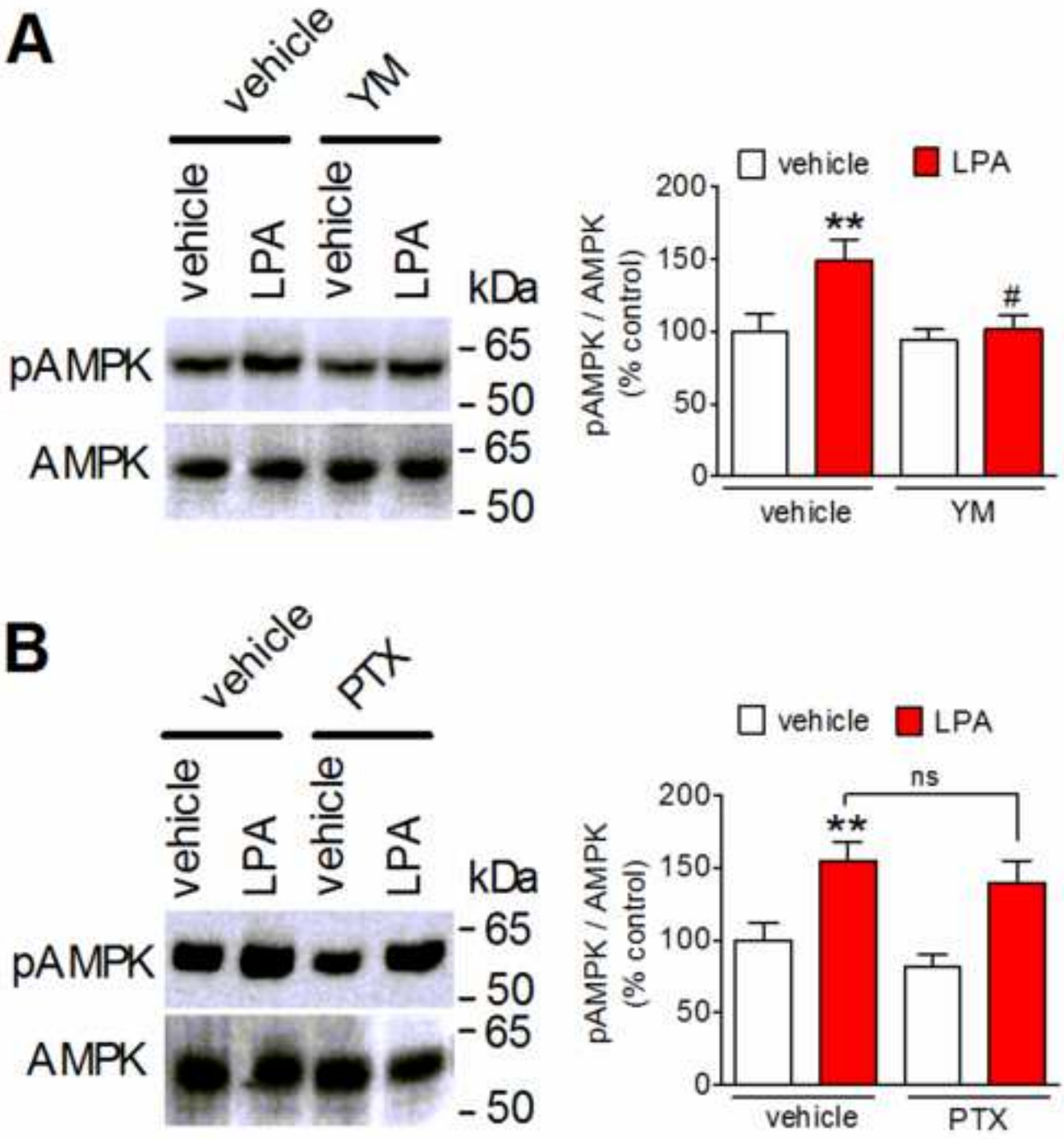

Fig. 6

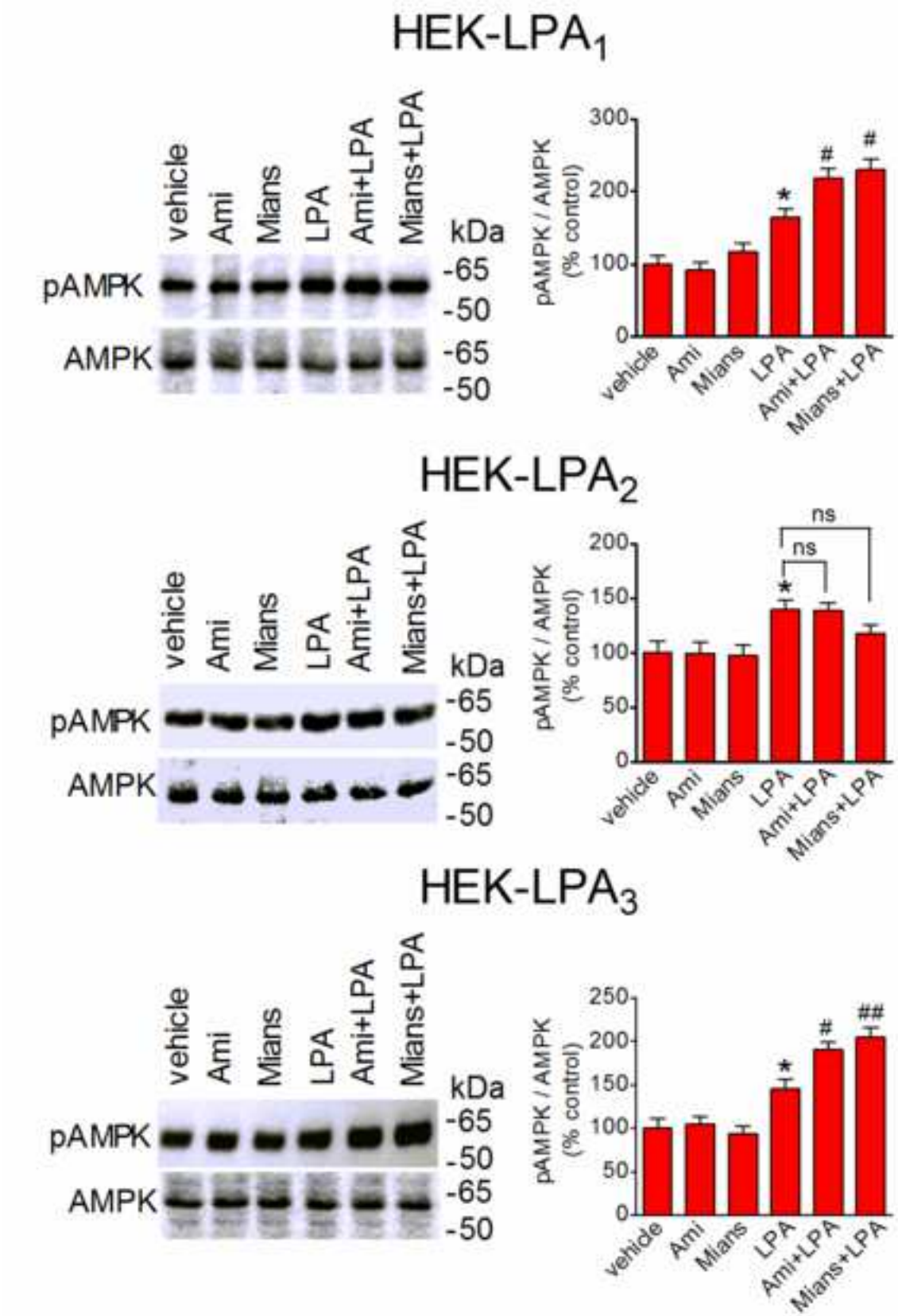

Fig.7

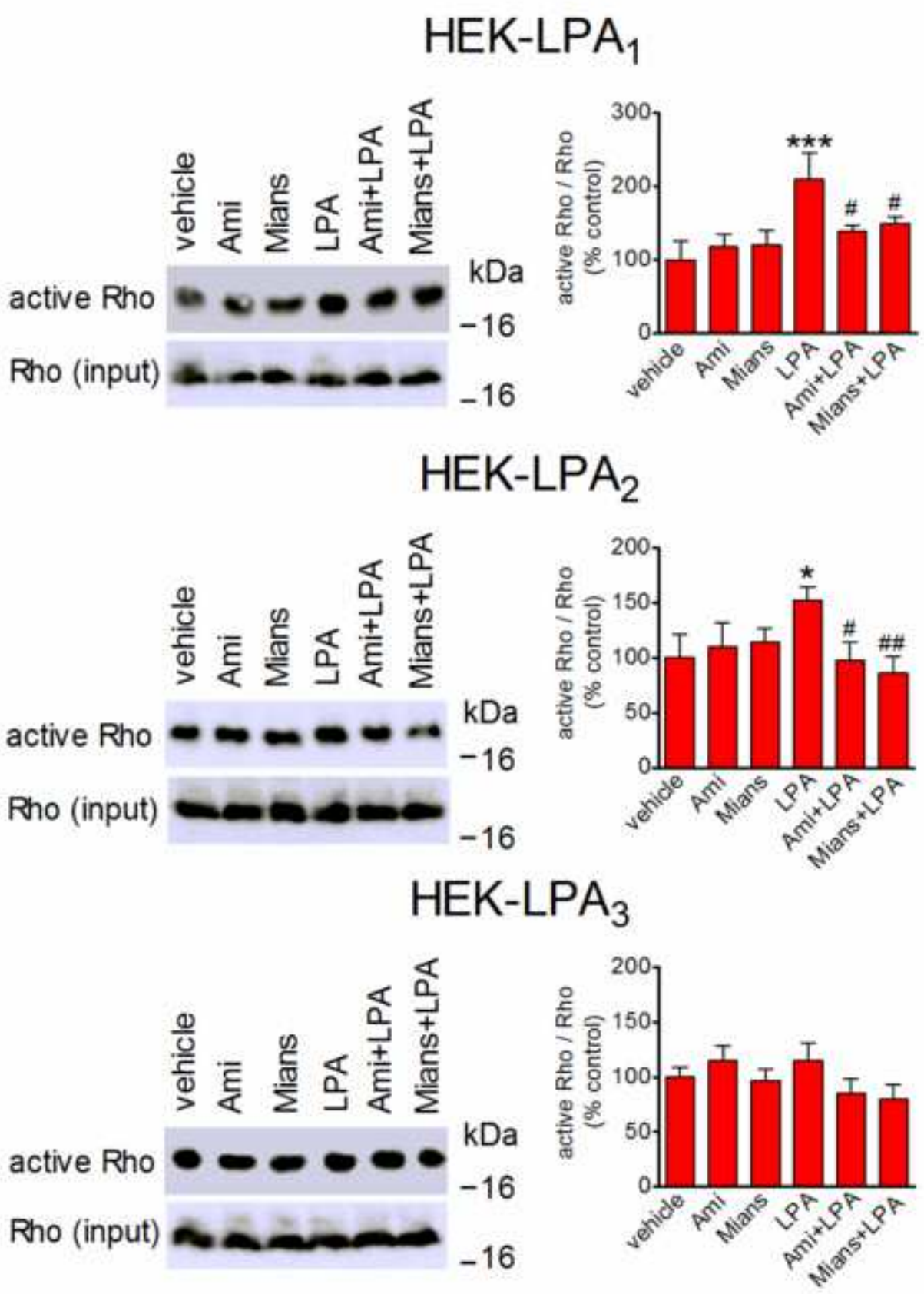

Fig. 8

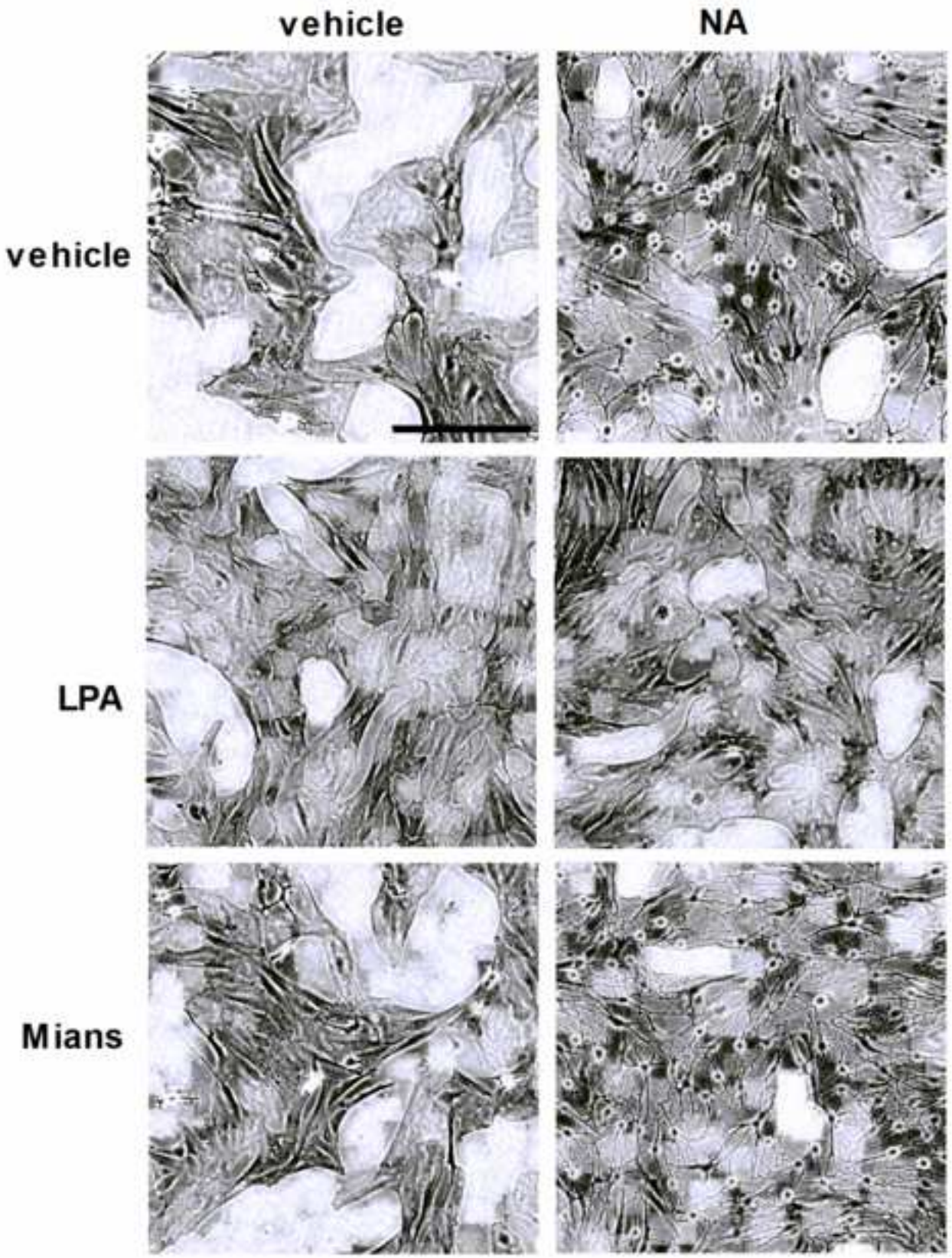

Fig. 9

Supplementary figures

Raw images